(Received 29 September 2025, Accepted 1 December 2025, Scheduled 24 December 2025)

Experimental Investigations of Pure Carbon Dioxide Splitting Using a Rod-Electrode-Type Microwave Plasma Source at Atmospheric Pressure

Hidenori Sekiguchi*

National Maritime Research Institute, National Institute of Maritime, Port and Aviation Technology
6-38-1, Shinkawa, Mitaka, Tokyo 181-0004, Japan

ABSTRACT: The purpose of this study is to experimentally investigate the applicability of a rod-electrode-type microwave plasma source (MPS) for pure carbon dioxide (CO_2) splitting at atmospheric pressure. This paper demonstrates that the rod-electrode-type MPS can convert pure CO_2 gas into plasma. The CO_2 splitting by the CO_2 plasma is investigated in terms of the pure CO_2 flow rate into the rod-electrode-type MPS and the average transmission power to the rod-electrode-type MPS. In the investigations, the emission spectrum of the CO_2 plasma is measured using a spectrometer to observe the dissociation reaction of the CO_2 gas, and the exhaust gas after the CO_2 plasma generation is analyzed using a mass spectrometer to evaluate the CO_2 conversion. As a result, the CO_2 conversion decreases with an increase in either the average transmission power to the rod-electrode-type MPS or the CO_2 flow rate into the rod-electrode-type MPS. Under the experimental conditions, the highest CO_2 conversion and energy efficiency are 6.3% and 3.7% at a specific energy input of 4.9 eV/molecule (equivalent to approximately 19.6 kJ/L), respectively.

1. INTRODUCTION

In recent decades, the progress of climate change, which is caused by increasing greenhouse gas (GHG) emissions into the atmosphere, has been a growing concern worldwide. The most considerable share in the GHGs is carbon dioxide (CO_2) gas. CO_2 gas is mainly emitted from the combustion of fossil fuels in the power generation, industrial, residential, and transport sectors [1]. Therefore, the emission of CO_2 gas into the atmosphere must be reduced to suppress climate change.

A promising approach to sustainably reduce the CO_2 concentration in the atmosphere is carbon capture, utilization and storage (CCUS), which includes CO_2 capture storage (CCS) [1] and CO_2 capture utilization (CCU) technologies [2]. In these technologies, CO_2 is first separated and captured from the emission source and the atmosphere by chemical absorption, physical absorption and adsorption, and membrane separation processes [1]. CCS stores captured CO_2 in the deep ocean and underground. CCU mainly synthesizes captured CO_2 to value-added products, including methanol, polymer, and urea [2]. The production of carbon monoxide (CO) gas from CO_2 gas is also an interest conversion, because CO is an essential feedstock in chemical industries [2]. For example, CO gas can be utilized for producing carbon-containing fuels by the Fischer-Tropsch process [3, 4] and chemicals such as organic acids, esters, alcohols, and aldehydes [5, 6]. In particular, the direct splitting of CO_2 gas into CO gas using renewable energy sources is useful for producing valuable electro-fuels and chemicals.

Recently, plasma technology has attracted attention for dissociating CO_2 gas, which is a highly stable molecule [7]. The primary plasma types for CO_2 splitting include dielectric barrier discharges, microwave discharges, and gliding arc discharges. Their plasmas can activate the electrons in CO_2 molecules via the generated discharge field. Additionally, microwave and gliding arc discharge plasmas can use most of the electron energy for the vibrational excitation of CO_2 molecules, and the vibration level plays an important role in the efficient splitting of CO_2 molecules. In particular, microwave discharge plasma can achieve high CO_2 conversion or energy efficiency under reduced pressure, although there is a trade-off between them [7–14]. However, the reduced pressure operation with a vacuum pump may not be suitable for industrial applications, resulting in a reduction in the energy efficiency of the entire system [14]. Therefore, the current focus of microwave discharge plasma for CO_2 splitting has shifted to the conversion and the energy efficiency at atmospheric pressure.

So far, several types of microwave discharge plasma have been experimentally investigated for CO_2 splitting at atmospheric pressure [14–18]. The microwave discharge plasma at atmospheric pressure is close to local thermodynamic equilibrium (LTE) [13]. The microwave power is typically transmitted to a resonator via a standard or tapered rectangular waveguide. The reactor generally consists of a coaxial or cylindrical resonator. In [14, 15], a combination of cylindrical and coaxial resonators has been used as a reactor via a standard rectangular waveguide. In addition, CO_2 gas is injected through tangential gas inlets, creating a swirling flow within the reactor. In [14], the pure CO_2 conversion and the energy efficiency are

* Corresponding author: Hidenori Sekiguchi (sekiguchi@m.mpat.go.jp).

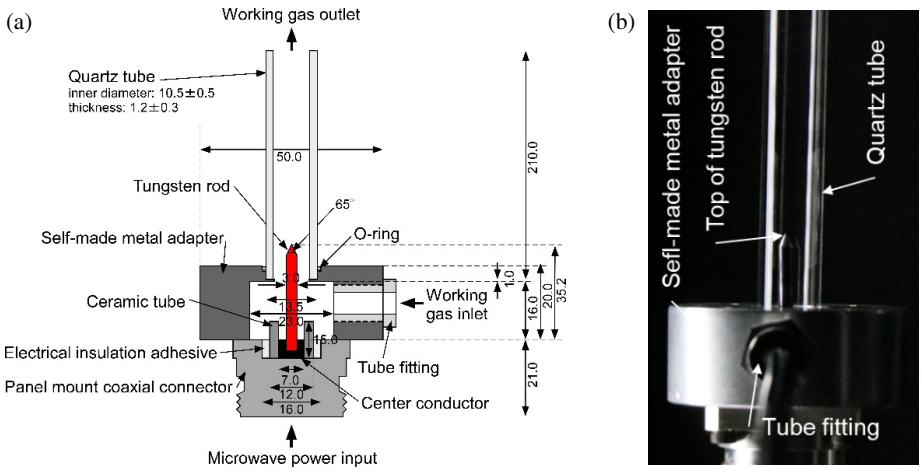

Structure diagram Photograph

FIGURE 1. Structure diagram and photograph of rod-electrode-type MPS.

approximately 14% and 22%, respectively. In [15], the pure CO_2 conversion of 8% is achieved at a specific energy input (SEI) of 1.5 eV/molecule, while the energy efficiency of about 25% is achieved at an SEI of 0.6 eV/molecule. Ref. [16] has reported a reactor consisting of a nozzle protruded from a standard rectangular waveguide. In the middle of the nozzle, a tungsten electrode is positioned to focus the microwaves. The reactor achieves the pure CO_2 conversion of approximately 9% at an SEI of 0.5 eV/molecule. Ref. [17] has presented the use of a commercial compact coaxial plasma torch powered by ultrafast microwave pulsation from an advanced solid-state microwave generator, achieving the energy efficiency of approximately 27% at an SEI of about 0.077 eV/molecule. As a side note, Ref. [18] has utilized a water-cooled Surfaguide device with a catalyst as a reactor, achieving the pure CO_2 conversion of approximately 45% at an SEI of 28 eV/molecule and the energy efficiency of approximately 20% at an SEI of about 1.5 eV/molecule. However, the use of thermal catalysts can be costly and require additional catalysts and electric power.

On the other hand, a rod-electrode-type microwave plasma source (MPS) has been developed for gas processing at atmospheric pressure [19–21]. The rod-electrode-type MPS uses a coaxial line instead of a conventional waveguide to supply the microwave power to the working gas, resulting in a simple and compact reactor. The microwave energy can be directly supplied to CO_2 gas from a rod electrode attached to a panel mound coaxial connector through the coaxial line. The compact rod-electrode-type MPS has the following advantages. It can be installed in a suitable location via a coaxial cable. Two or more rod-electrode-type MPSs can be parallelized using a coaxial distributor from a high-power magnetron. Therefore, the rod-electrode-type MPS will be reasonable for practical applications. On the other hand, to the author's knowledge, there are no studies on the pure CO_2 splitting using rod-electrode-type MPS with its unique structure. The investigation of its applicability is crucial for the effective use of CO_2.

The purpose of this study is to experimentally investigate the applicability of a rod-electrode-type MPS for pure CO_2 splitting without the use of catalysts and additional gases at atmospheric pressure. The experimental investigations ultimately focus on evaluating the CO_2 conversion, SEI, and energy efficiency in terms of the pure CO_2 gas flow rate into the rod-electrode-type MPS and the average transmission power to the rod-electrode-type MPS.

2. EXPERIMENT

2.1. Experimental System and Method

Figure 1 shows the structure diagram and photograph of a rod-electrode-type MPS in this study. The basic structure has been reported in detail in the previous literature [19–21]. The sizes of the parts and materials are shown in millimeters (mm) in Fig. 1(a). In the rod-electrode-type MPS, the working gas can flow around the tungsten rod in the quartz tube, and the tungsten rod can directly supply the microwave energy to the working gas. Here, it is noted in Fig. 1(b) that the photograph is slightly tilted by the camera position.

Figure 2 shows the schematic diagram of the experimental system for the pure CO_2 splitting using the rod-electrode-type

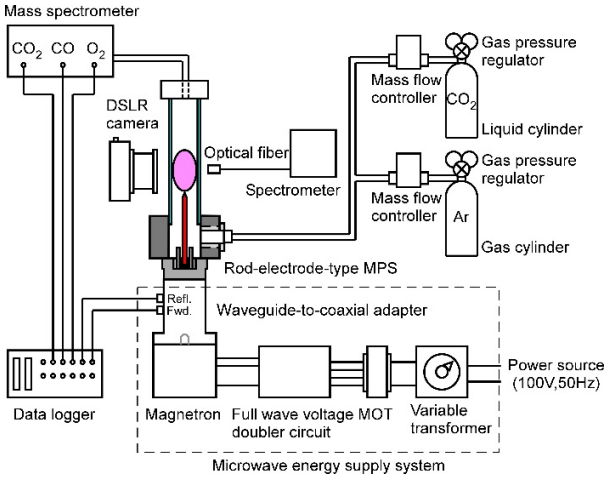

FIGURE 2. Schematic diagram of experimental system.

MPS. In this study, argon (Ar) and CO_2 gases were used as the working gas. Their flow rates were controlled by the mass flow controllers under the standard ambient temperature and pressure (SATP) of 298.15 K and 101.325 kPa.

The microwave energy supply system, digital single-lens reflex (DSLR) camera, and spectrometer used in this study have been described in detail in the previous literature [19–21]. The experiments were conducted in a dark room to observe the emission of light from the plasma. Here, the head of the optical fiber was then positioned at a height of 5 mm and a horizontal distance of 30 mm from the tip of the tungsten rod. The DSLR camera was used to capture the plasma, and the spectrometer was used to investigate the dissociation reaction in the CO_2 plasma.

In addition, a mass spectrometer (V&F Analyze-und Messtechnik GmbH, CombiSense) was used to analyze the exhaust gas after the CO_2 plasma generation. The mass spectrometer used can measure the concentrations of the target components between 0 and 100 vol% with an accuracy of $< \pm 2\%$ using a suction flow rate of about 0.2 L/min. It can output the analog voltages corresponding to the concentrations of the measured target components. Here, mass spectrometers have often been used to measure the concentration of CO_2 [10, 14–16, 22].

In the end, the data logger with a sampling period of 1 µs (Graphtec Corporation, GL980) was used to record the forward and reflection voltages at the input port of the rod-electrode-type MPS detected by the waveguide-to-coaxial adapter and the analog voltages corresponding to the concentrations of the target components measured by the mass spectrometer. The forward and reflection voltages were converted to the corresponding powers using the correction function of the waveguide-to-coaxial adapter. The transmission power to the rod-electrode-type MPS was calculated by subtracting the reflection power from the forward power.

In the experiments, first, only Ar gas with a flow rate of 0.3 L/min was fed into the rod-electrode-type MPS. By increasing the forward power to the rod-electrode-type MPS, only Ar gas was converted into plasma through autoignition near the tip of the tungsten rod in the quartz tube. Second, CO_2 gas with a specific flow rate was added into the Ar plasma, and the Ar/CO_2 plasma was generated in the rod-electrode-type MPS. The Ar plasma then acts as an electron source stimulating the vibrational excitation of the CO_2 molecule. The vibrational excitation can convert CO_2 into plasma. Finally, the Ar gas was shut off and only pure CO_2 gas was converted into plasma. Namely, the Ar gas was used only for the plasma ignition in the rod-electrode-type MPS. As a side note, noble gases such as Ar are known to be easily converted into plasma. The pure CO_2 gas could not be converted directly into plasma through autoignition in the experiments, because CO_2 has a higher dielectric breakdown voltage than Ar. In the subsequent experiments, the average transmission power was in the range of about 90 to 150 W, and the CO_2 flow rate was in the range of 0.3 to 0.9 L/min.

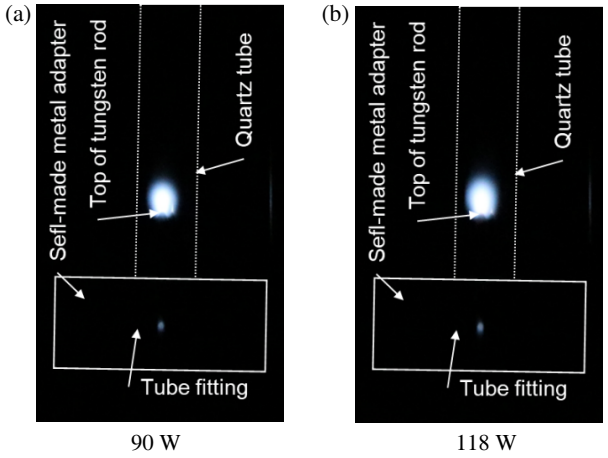

FIGURE 3. Capture images of CO_2 plasmas generated by average transmission powers of approximately 90 W and 118 W at flow rate of 0.3 L/min.

2.2. Evaluation Method of CO_2 Splitting

A pure CO_2 splitting occurs commonly according to the endothermic reaction of Eq. (1).

$$CO_2 \rightarrow CO + \frac{1}{2}O_2, \quad \Delta H = 283.3\,[\text{kJ/mol}], \tag{1}$$

where ΔH is the reaction enthalpy at the SATP. On the other hand, the pure CO_2 splitting can occur according to the endothermic reaction of Eq. (2), but it has been found to be a challenging reaction from the literatures [8, 12].

$$CO_2 \rightarrow C + O_2, \quad \Delta H = 395.4\,[\text{kJ/mol}]. \tag{2}$$

Therefore, the exhaust gas after the CO_2 plasma generation may contain CO_2, CO, and oxygen molecule (O_2) due to the CO_2 splitting of Eq. (1). In the experiments, the CO_2, CO, and O_2 concentrations in the exhaust gas can be analyzed using the mass spectrometer. The CO_2 conversion χ_{CO_2}% can be then calculated from the CO_2 concentration $CO_{2\_vol\%}$ vol%, taking into account the gas expansion after the CO_2 splitting of Eq. (1) [15].

$$\chi_{CO_2}\,[\%] = \frac{100\,[\text{vol\%}] - CO_{2\_VOL\%}\,[\text{vol\%}]}{100\,[\text{vol\%}] + \frac{1}{2}CO_{2\_VOL\%}\,[\text{vol\%}]} \times 100. \tag{3}$$

Here, the unit of vol% stands for percent by volume. The SEI kJ/L can be calculated from the transmission power TP_{ave} kW to the rod-electrode-type MPS and the CO_2 gas flow rate CO_{2_flow} L/min into the rod-electrode-type MPS.

$$SEI\left[\frac{\text{kJ}}{\text{L}}\right] = \frac{TP_{ave}\,[\text{kW}]}{CO_{2\_flow}\left[\frac{\text{L}}{\text{min}}\right]} \times 60\left[\frac{\text{s}}{\text{min}}\right]. \tag{4}$$

The SEI eV/molecule can also be defined as the electron volt (eV) per CO_2 molecule:

$$SEI\left[\frac{\text{eV}}{\text{molecule}}\right] = SEI\left[\frac{\text{kJ}}{\text{L}}\right] \times \frac{1000}{\text{eV}\left[\frac{\text{J}}{\text{eV}}\right]} \times \frac{V_m\left[\frac{\text{L}}{\text{mol}}\right]}{N_A\left[\frac{\text{molecule}}{\text{mol}}\right]}, \tag{5}$$

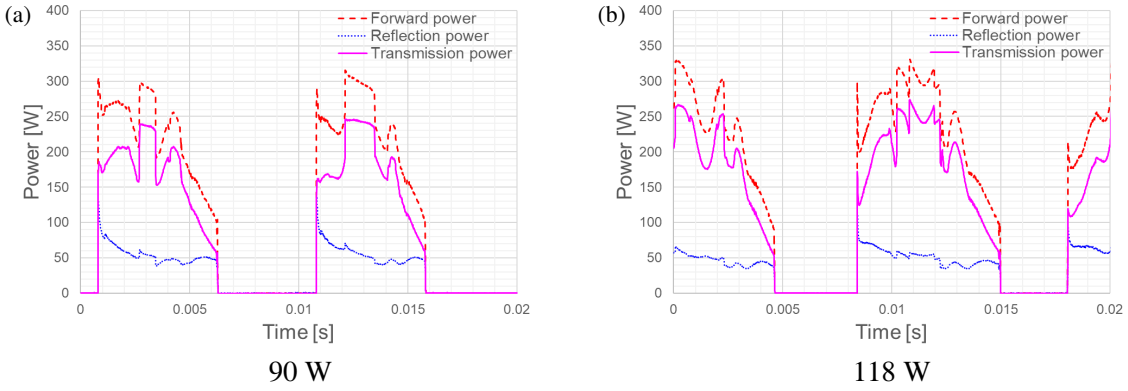

FIGURE 4. Forward, reflection, and transmission power waveforms corresponding to Fig. 3 at the input port of the rod-electrode-type MPS.

where 1 eV is equal to the energy about 1.602×10^{-19} J; V_m is the molar volume of about 24.45 L/mol at the SATP; and N_A is the Avogadro constant about 6.022×10^{23} molecule/mol. The energy efficiency η% can be defined as:

$$\eta\,[\%] = \frac{\Delta H\left[\frac{\text{kJ}}{\text{mol}}\right] \times \chi_{CO_2}\,[\%]}{SEI\left[\frac{\text{kJ}}{\text{L}}\right] \times V_m\left[\frac{\text{L}}{\text{mol}}\right]} \tag{6}$$

Eqs. (3)–(6) can evaluate the effects of the pure CO_2 splitting of Eq. (1) in the experiments.

3. RESULTS AND DISCUSSION

3.1. Generation and Spectrum of CO_2 Plasma

Figure 3 shows the capture images of the CO_2 plasmas generated by the average transmission powers of about 90 W and 118 W at the flow rate of 0.3 L/min into the rod-electrode-type MPS. These images were taken at the same viewing angle as Fig. 1(b) in a dark room. The white solid and dashed lines show the outlines of the self-made metal adapter and the quartz tube, respectively. In Figs. 3(a) and (b), the CO_2 plasma can be confirmed to be generated at the tip of the tungsten rod in the quartz tube. It may be operating as a diffuse discharge due to the properties of the CO_2 gas. The CO_2 plasma had two distinct regions: a whitish-bright region near the tip of the tungsten rod and a bluish-dimmer region around the whitish-bright region. These regions of the CO_2 plasma slightly expanded with the increase in the average transmission power. According to the literature [23], the whitish-bright region has a high-temperature, where CO_2 molecules dissociate into CO molecules and oxygen atoms (O atoms). On the contrary, the bluish-dimmer region has a relatively low-temperature, where CO molecules and O atoms recombine into CO_2 molecules.

After the experiments, the tip of the tungsten rod was visually observed to remain the same shape but turn white. The white discoloration is probably caused by the oxidation of the tungsten due to exposure to oxygen radicals. The tungsten rod with the whitened tip could be used subsequently for the CO_2 plasma generation.

Figure 4 shows the forward, reflection, and transmission power waveforms corresponding to Fig. 3 at the input port of the rod-electrode-type MPS. In Figs. 4(a) and (b), the period of these waveforms was approximately 0.01 s, because the full wave voltage doubler circuit was used in the microwave energy supply system. This means that the CO_2 plasma actually turns on and off in a 0.01-second period, although it appeared to be a very stable small flame. The power waveforms were complex due to the electrical characteristics of the CO_2 plasma, the rod-electrode-type MPS, and the microwave energy supply system. Incidentally, the radiated power density leaked from the CO_2 plasma was lower than 5 mW/cm^2 in all experiments. Namely, the transmission power contained the slight radiated power to the CO_2 plasma generation power. The average transmission powers were calculated as the mean values of the transmission power during the 10 second period. The power transmission efficiencies were then about 70% in Figs. 4(a) and (b). The power transmission efficiency can be improved by adjusting the length of the tungsten rod from the previous literature [19].

Figure 5 shows the spectra of the CO_2 plasmas corresponding to Fig. 3. Some emission peaks can be commonly observed in the spectra of the CO_2 plasmas. The emission peaks at the wavelengths of 248 nm and 777 nm were identified as the typical carbon and oxygen neutral lines. From the literature [16], the emission peaks at the wavelengths of 473 nm and 516 nm were identified as the C_2 Swan band system. According to the literature [23], a broadband continuum emission in the wavelength range of about 300–700 nm is attributed to the recombination processes of CO + O and/or O + O. So, the emission spectra imply the dissociation reaction of the CO_2 gas. Furthermore, no solid carbon deposition was observed in the rod-

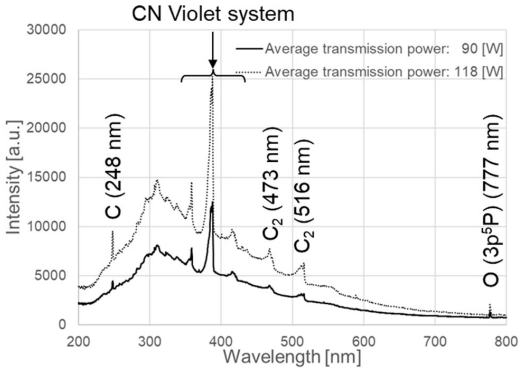

FIGURE 5. Spectra of CO_2 plasma corresponding to Fig. 3.

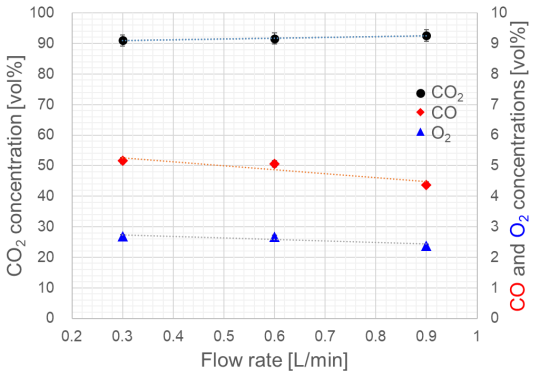

FIGURE 6. Relationships of CO_2, CO, and O_2 concentrations in exhaust gas after CO_2 plasma generation to flow rates of 0.3, 0.6, and 0.9 L/min into rod-electrode-type MPS at almost the same average transmission power to rod-electrode-type MPS. Error bars represent the accuracy of measured concentrations, and invisible error bars indicate values smaller than the symbol.

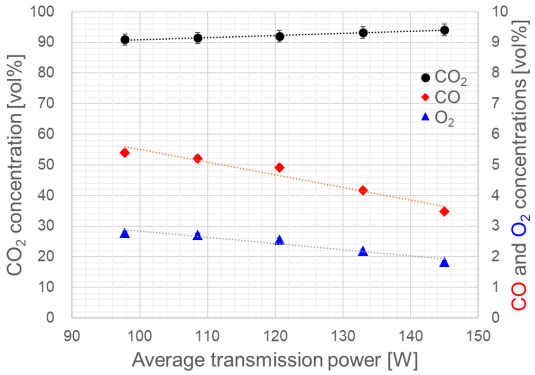

FIGURE 7. Relationships of CO_2, CO, and O_2 concentrations in exhaust gas after CO_2 plasma generation to average transmission powers to rod-electrode-type MPS at flow rate of 0.3 L/min into rod-electrode-type MPS. Error bars represent the accuracy of measured concentrations, and invisible error bars indicate values smaller than the symbol.

electrode-type MPS after the experiments, similar to the results of [8, 12] on the CO_2 splitting using microwave plasma. As a result, the CO_2 plasma in the rod-electrode-type MPS can be expected to have the CO_2 splitting of Eq. (1). Here, the emission peaks in the wavelength range of about 350–430 nm coincided with the CN Violet system. The CN Violet system may be caused by nitrogenous compounds as impurities in the CO_2 liquid cylinder with a purity of $\geq 99.5\%$.

3.2. CO_2, CO, O_2 Concentrations in Exhaust Gas after the CO_2 Plasma Generation

Figure 6 shows the relationships of the CO_2, CO, and O_2 concentrations in the exhaust gas after the CO_2 plasma generation to the CO_2 flow rates of 0.3, 0.6, and 0.9 L/min into the rod-electrode-type MPS. The CO_2, CO, and O_2 concentrations were indicated as the mean values of 1,000,000 measurements over a 10-second period. Here, the average transmission power to the rod-electrode-type MPS was set to be almost the same, although the forward and reflection powers varied with the CO_2 flow rate. As a result, the CO_2 concentration increased and the CO and O_2 concentrations decreased with the increase in the CO_2 flow rate. Under the experimental conditions, the CO_2 concentration was lowest at the CO_2 flow rate of 0.3 L/min. On other words, the CO_2 conversion increases with the decrease in the CO_2 flow rate.

On the other hand, the increase in the CO_2 flow rate results in the increase in the flow velocity in the quartz tube. It decreases the CO_2 dissociation time in the CO_2 plasma region, and increases the non-dissociative CO_2 flow volume outside the CO_2 plasma region. Therefore, the diameter of the quartz tube should be essentially matched to the width of the plasma to reduce the non-dissociative CO_2 flow volume outside the CO_2 plasma region in the near future.

Next, Fig. 7 shows the relationships of the CO_2, CO, and O_2 concentrations in the exhaust gas after the CO_2 plasma generation to the average transmission powers to the rod-electrode-type MPS at the CO_2 flow rate of 0.3 L/min into the rod-electrode-type MPS. As a result, the CO_2 concentration increased and the CO and O_2 concentrations decreased with the increase in the average transmission power. At each average transmission power, the sum of the CO_2, CO, and O_2 concentrations was between 99.1% and 99.6% despite the measurement accuracy of $< \pm 2\%$. Also, the ratio of the CO concentration to the O_2 concentration was approximately 1.9. Namely, the CO_2, CO, and O_2 concentrations were measured with high accuracy, and were almost in accordance with Eq. (1). The increase in the CO_2 concentration may be caused by the fact that the low-temperature region increased relative to the high-temperature region in the expansion of the CO_2 plasma with the increase in the average transmission power, as described in Subsection 3.1. Namely, the region where CO molecules and O atoms recombine into CO_2 molecules may have increased relative to the region where CO_2 molecules dissociate into CO molecules and O atoms.

3.3. Evaluations of CO_2 Splitting

The effects of the pure CO_2 splitting in the experiments were evaluated by the CO_2 conversion, the SEI, and the energy efficiency, based on Subsection 2.2. Fig. 8 shows the relationship

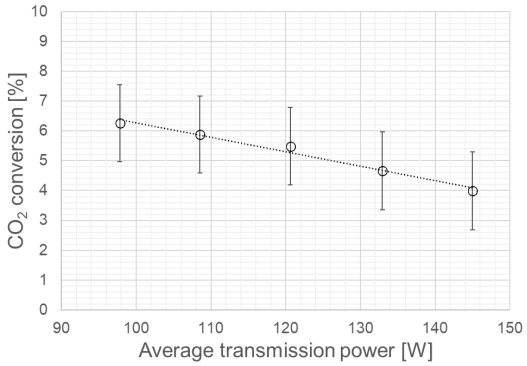

FIGURE 8. Relationship of CO_2 conversions to average transmission powers to rod-electrode-type MPS at CO_2 flow rate of 0.3 L/min into rod-electrode-type MPS. Error bars are calculated from Eq. (3) taking into account the accuracy of measured CO_2 concentration.

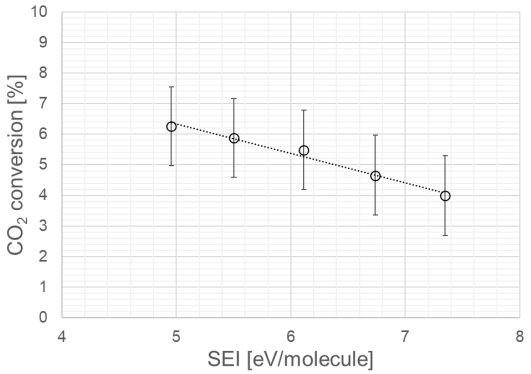

FIGURE 9. Relationship of CO_2 conversions to SEIs, corresponding to Fig. 8. Error bars are calculated from Eq. (3) taking into account the accuracy of measured CO_2 concentration.

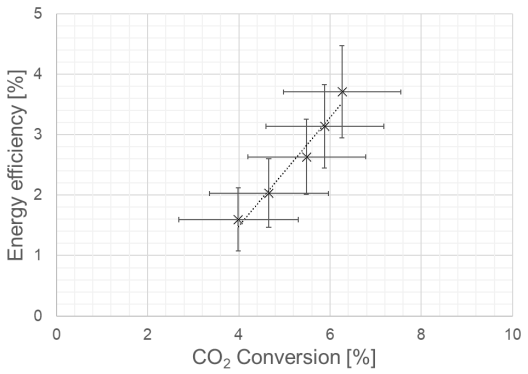

FIGURE 10. Relationship of energy efficiencies to CO_2 conversions, corresponding to Fig. 8. Error bars are calculated from Eq. (3) and (6) taking into account the accuracy of measured CO_2 concentration.

of the CO_2 conversions to the average transmission powers to the rod-electrode-type MPS, corresponding to Fig. 7. As expected, the CO_2 conversion decreased with the increase in the average transmission power to the rod-electrode-type MPS. The highest CO_2 conversion was 6.3% at the average transmission power of 97.8 W.

Figure 9 shows the relationship of the CO_2 conversions to the SEIs, and Fig. 10 shows the energy efficiencies to the CO_2 conversions, corresponding to Fig. 8. From Fig. 9, the highest CO_2 conversion was 6.3% at the SEI of 4.9 eV/molecule (equivalent to approximately 19.6 kJ/L from Eq. (4)). From Fig. 10, the highest energy efficiency was 3.7% at the highest CO_2 conversion of 6.3%. Namely, the highest CO_2 conversion and energy efficiency achieved at the same SEI. However, the highest CO_2 conversion and energy efficiency were lower than those in [14–17]. The reason may be due to the quenching effect of the CO_2 plasma. According to the literatures [7, 8, 11, 13], the quenching of the CO_2 plasma is effective in suppressing the recombination reactions between the CO molecules and O atoms produced in the CO_2 plasma, thereby enhancing the CO_2 conversion and the energy efficiency. Therefore, the rod-electrode-type MPS will be improved to enhance the quenching effect in the near future. The quenching in the rod-electrode-type MPS may be achieved by inducing swirl flow [14, 15], incorporating cooling mechanism [14–16], and applying pulsed power [17]. The improvements are currently under consideration.

4. CONCLUSIONS

This paper has demonstrated that the rod-electrode-type MPS can convert pure CO_2 gas into plasma, in terms of CO_2 splitting at atmospheric pressure. Some of the pure CO_2 gas was split into CO and O_2 gases after the CO_2 plasma generation. The CO_2 conversion decreased with the increase in either the average transmission power to the rod-electrode-type MPS or the CO_2 flow rate into the rod-electrode-type MPS. The highest CO_2 conversion of 6.3% and energy efficiency of 3.7% were achieved at the SEI of 4.9 eV/molecule (equivalent to approximately 19.6 kJ/L). The results indicated that a rod-electrode-type MPS was applicable to pure CO_2 splitting at atmospheric pressure. However, the highest CO_2 conversion and energy efficiency were lower than those in the conventional microwave plasma systems.

In the future study, the rod-electrode-type MPS will be improved to increase the CO_2 conversion and energy efficiency. The diameter of the quartz tube will be matched to the width of the plasma to reduce the non-dissociative CO_2 flow volume outside the CO_2 plasma region. The quenching mechanism of the CO_2 plasma will be incorporated into the rod-electrode-type MPS. Besides, the length of the tungsten rod will be adjusted to increase the power transmission efficiency. The effects will be discussed in the future.

ACKNOWLEDGEMENT

This work was supported in part by the Japan Society for the Promotion of Science (JSPS) KAKENHI Grant Number 21K04521.

REFERENCES

[1] IPCC, *IPCC Special Report on Carbon Dioxide Capture and Storage*, Cambridge University Press, 2005.

[2] Kim, C., C.-J. Yoo, H.-S. Oh, B. K. Min, and U. Lee, "Review of carbon dioxide utilization technologies and their potential for industrial application," *Journal of CO2 Utilization*, Vol. 65, 102239, 2022.

[3] Ail, S. S. and S. Dasappa, "Biomass to liquid transportation fuel via Fischer Tropsch synthesis — Technology review and current scenario," *Renewable and Sustainable Energy Reviews*, Vol. 58, 267–286, 2016.

[4] Loosdrecht, Van de J., F. G. Botes, I. M. Ciobica, A. Ferreira, P. Gibson, D. J. Moodley, A. M. Saib, J. L. Visagie, C. J. Weststrate, and J. W. Niemantsverdriet, "Fischer-tropsch synthesis: Catalysts and chemistry," *Comprehensive Inorganic Chemistry II*, Vol. 7, 525–557, 2013.

[5] Lahijani, P., Z. A. Zainal, M. Mohammadi, and A. R. Mohamed, "Conversion of the greenhouse gas CO_2 to the fuel gas CO via the Boudouard reaction: A review," *Renewable and Sustainable Energy Reviews*, Vol. 41, 615–632, 2015.

[6] Peng, J.-B., H.-Q. Geng, and X.-F. Wu, "The chemistry of CO: Carbonylation," *Chem*, Vol. 5, No. 3, 526–552, 2019.

[7] Snoeckx, R. and A. Bogaerts, "Plasma technology — A novel solution for CO_2 conversion?" *Chemical Society Reviews*, Vol. 46,

No. 19, 5805–5863, 2017.

[8] Bogaerts, A. and G. Centi, "Plasma technology for CO_2 conversion: A personal perspective on prospects and gaps," *Frontiers in Energy Research*, Vol. 8, 1–23, 2020.

[9] Bogaerts, A. and E. C. Neyts, "Plasma technology: An emerging technology for energy storage," *ACS Energy Letters*, Vol. 3, No. 4, 1013–1027, 2018.

[10] Qin, Y., G. Niu, X. Wang, D. Luo, and Y. Duan, "Status of CO_2 conversion using microwave plasma," *Journal of CO2 Utilization*, Vol. 28, 283–291, 2018.

[11] Yin, Y., T. Yang, Z. Li, E. Devid, D. Auerbach, and A. W. Kleyn, "CO_2 conversion by plasma: How to get efficient CO_2 conversion and high energy efficiency," *Physical Chemistry Chemical Physics*, Vol. 23, No. 13, 7974–7987, 2021.

[12] Centi, G., S. Perathoner, and G. Papanikolaou, "Plasma assisted CO_2 splitting to carbon and oxygen: A concept review analysis," *Journal of CO2 Utilization*, Vol. 54, 101775, 2021.

[13] Fridman, A., *Plasma Chemistry*, Cambridge University Press, 2008.

[14] Kiefer, C. K., R. Antunes, A. Hecimovic, A. Meindl, and U. Fantz, "CO_2 dissociation using a lab-scale microwave plasma torch: An experimental study in view of industrial application," *Chemical Engineering Journal*, Vol. 481, 148326, 2024.

[15] Wiegers, K., A. Schulz, M. Walker, and G. E. M. Tovar, "Determination of the conversion and efficiency for CO_2 in an atmospheric pressure microwave plasma torch," *Chemie Ingenieur Technik*, Vol. 94, No. 3, 299–308, 2022.

[16] Mitsingas, C. M., R. Rajasegar, S. Hammack, H. Do, and T. Lee, "High energy efficiency plasma conversion of CO_2 at atmospheric pressure using a direct-coupled microwave plasma system," *IEEE Transactions on Plasma Science*, Vol. 44, No. 4, 651–656, 2016.

[17] Soldatov, S., G. Link, L. Silberer, C. M. Schmedt, E. Carbone, F. D'Isa, J. Jelonnek, R. Dittmeyer, and A. Navarrete, "Time-resolved optical emission spectroscopy reveals nonequilibrium conditions for CO_2 splitting in atmospheric plasma sustained with ultrafast microwave pulsation," *ACS Energy Letters*, Vol. 6, No. 1, 124–130, 2021.

[18] Spencer, L. F. and A. D. Gallimore, "CO_2 dissociation in an atmospheric pressure plasma/catalyst system: A study of efficiency," *Plasma Sources Science and Technology*, Vol. 22, 015019, 2013.

[19] Sekiguchi, H., "Study on development of rod-electrode-type microwave plasma source at atmospheric pressure," *Progress In Electromagnetics Research C*, Vol. 160, 113–119, 2025.

[20] Sekiguchi, H., "Pure ammonia direct decomposition using rod-electrode-type microwave plasma source," *International Journal of Hydrogen Energy*, Vol. 57, 1010–1016, 2024.

[21] Sekiguchi, H., "Experimental investigations of plasma-assisted ammonia combustion using rod-electrode-type microwave plasma source," *International Journal of Hydrogen Energy*, Vol. 65, 66–73, 2024.

[22] D'Isa, F. A., E. A. D. Carbone, A. Hecimovic, and U. Fantz, "Performance analysis of a 2.45 GHz microwave plasma torch for CO_2 decomposition in gas swirl configuration," *Plasma Sources Science and Technology*, Vol. 29, No. 10, 105009, 2020.

[23] Uhm, H. S., H. S. Kwak, and Y. C. Hong, "Carbon dioxide elimination and regeneration of resources in a microwave plasma torch," *Environmental Pollution*, Vol. 211, 191–197, 2016.